THE MASS AND GEOMETRY OF THE COSMOS

CHARLES HELLABY (PRESENTER)
Department of Mathematics and Applied Mathematics
University of Cape Town
E-mail: cwh@maths.uct.ac.za

HUI-CHING LU
Department of Mathematics and Applied Mathematics
University of Cape Town
E-mail: hclu@maths.uct.ac.za

As the cosmological data generated by redshift surveys becomes increasingly accurate, the proper reduction and interpretation of the high redshift data will require knowledge of the cosmic geometry that is traveled through by the light rays we observe. It will no longer be necessary to assume homogeneity, the data will make it possible to quantify the level of homogeneity on different scales. The ultimate application of Einsteins field equations is to determine the relation between matter and geometry in the real universe. A set of observations of the redshifts, angular diameters, and apparent luminosities of galaxies, as well as their number counts, combined with knowledge of their true diameters, luminosities and masses, plus the cosmic equation of state, can be turned into metric information. Though much theoretical development has been done, the proposed methods have never been implemented, so the 2 key issues of choosing appropriate numerical methods and handling real observational data have not been addressed. A preliminary numerical reduction scheme has been written and tested. The methods and difficulties encountered will be discussed. The locus where the past null cone crosses the apparent horizon has significant theoretical, numerical and observational properties. It allows us to determine a characteristic mass of the cosmos that is quite model independent.

1. Obtaining the Metric of the Cosmos from Observations

1.1. *Introduction*

Large-scale automated redshift surveys, such as SDSS, 2dF, 6dF, etc, are opening up new possibilities for measuring the content and dynamics of the universe.

Given sufficiently accurate and complete galaxy data on our past null cone (PNC), viz redshifts, apparent luminosities and/or angular diameters, and number counts in redshift space, and given the source properties, viz absolute luminosities and/or true diameters, and source masses, plus an assumption about the cosmic equation of state, we can determine the metric of our cosmos — the geometry of the spacetime we live in.

The primary measures of cosmic distance are the diamter distance

$$d_D = R = \frac{D}{\delta} = \frac{\text{true diameter}}{\text{angular diameter}}$$

and the luminosity distance

$$d_L = \sqrt{\frac{L}{\ell}}\, d_{10} = \sqrt{\frac{\text{absolute luminosity}}{\text{apparent luminosity}}} \times 10 \text{ pc}$$

of sources. The density in redshift space is

$$mn = \text{mass per source} \times \text{number density in } z \text{ space}$$

where the number density per steradian per unit redshift interval, n, is dimensionless. Note that the observables are δ, ℓ, n, and that each one is multiplied of divided by a source property D, L, m. Since galaxy properties change with time, these source evolution functions must be known, for example from a theory of galaxy evolution.

1.2. *Observer's Past Null Cone*

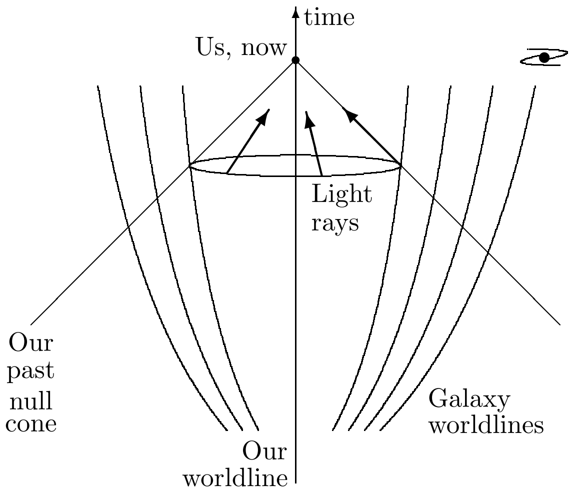

Several things affect a source's appearance, so if far away objects look different, is it because of

- Cosmic evolution (EFEs): the equation of state determines the scale factor evolution which determines redshift down the null cone,

$$p(\rho) \quad \rightarrow \quad S(t) \quad \rightarrow \quad z$$

- Source evolution: the same type of object looks different long ago (at large z) than recently (small z),

$$L = L(t)\ ,\quad D = D(t)\ ,\quad m = m(t) \qquad \rightarrow \qquad L = L(z)\ ,\quad D = D(z)\ ,\quad m = m(z)$$

• or Inhomogeneity: spatial variation makes source properties different far away (large z) and nearby (small z),

$$L = L(r) \ , \quad D = D(r) \ , \quad m = m(r) \quad \rightarrow \quad \rho = \rho(t, r)$$

1.3. *How Homogeneous?*

The conventional wisdom is that the Copernican principle ensures homogeneity on very large scales, but this scale still not well defined, and homogeneity in fact *assumed.* This assumption has been essential up to now, and has served us well. But now we're getting all this data, we won't have to assume it much longer, and we should rather try to prove (or disprove) homogeneity. Indeed we should quantify it — how close to homogeneity are we on a variety of scales?

To do this, we must analyse observational data *without* assuming homogeneity, and here lies a significant problem because so much of the current analysis does assume it. There's a danger of a circular argument. Isotropy about the obsever can be established with no assumptions about the correct cosmological model. Radial variation that is hard to separate

The two key papers that considered the problem of obtaining geometry from cosmological observations are "Observations in Cosmology" by Kristian and Sachs[1] and "Ideal Observational Cosmology" by Ellis, Nel, Maartens, Stoeger and Whitman[2]. For a list of references and some details of earlier work, see[3]. The algorithm we shall be using was given by Mustapha, Hellaby and Ellis[4].

1.4. *Lemaître-Tolman model (LT)*

To get the investigation going, we start with simplest case - the simplest inhomogeneous cosmology. The LT model is spherically symmetric, having only radial variation, and it evolves with time. The metric is[5,6,7,8]

$$ds^2 = -dt^2 + \frac{(R')^2}{1+2E}\, dr^2 + R^2\, d\Omega^2$$

$$\text{where} \qquad d\Omega^2 = d\theta^2 + \sin^2\theta\, d\phi^2 \qquad \text{and} \qquad {}' \equiv \partial/\partial r \ .$$

Here $R = R(t, r)$ is the areal radius, which equals the diameter distance, and $E = E(r) \geq -1/2$ is an arbitrary function that represents local geometry. It has a dust equation of state, $T^{ab} = \rho u^a u^b$ and the coordinates are comoving with the matter, $u^a = \delta^a_t$. From the Einstein field equations we obtain the density and the evolution DE

$$\kappa\rho(t, r) = \frac{2M'}{R^2 R'} \ , \qquad \dot{R}^2 = \frac{2M}{R} + 2E + \frac{\Lambda R^2}{3} \ , \qquad \text{where} \qquad \dot{} \equiv \partial/\partial t$$

where Λ is the cosmological constant, and the second arbitrary function $M = M(r)$ gives the gravitational mass interior to the comoving shell at r. We see that $E(r)$

also represents local energy per unit mass of worldlines. The solution depends on E, and for the hyperbolic case $E > 0$ it is

$$R = \frac{M}{2E}(\cosh\eta - 1) \ , \qquad (\sinh\eta - \eta) = \frac{(2E)^{3/2}(t - t_B)}{M}$$

and $t_B = t_B(r)$ is the third arbitrary function that gives the local time of big bang. The parabolic and elliptic solutions are similar.

1.5. *Integrating Down the PNC*

The observer's past null cone is null and radial, i.e. it obeys

$$\frac{dt}{dr} = -\frac{R'}{\sqrt{1+2E}} = \hat{t}'$$

We write the solution, the PNC locus, as $t = \hat{t}(r)$, so that the diameter and luminosity distances are $d_D = \hat{R} = R(\hat{t}(r), r)$, $d_L = d_D(1+z)^2$ and the redshift is

$$(1+z) = \int_{PNC} \frac{\dot{R}'}{\sqrt{1+2E}} \, dr$$

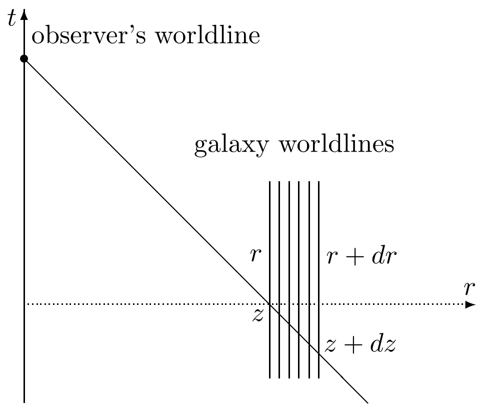

The number density in z-space is

$$\begin{aligned} m\,n\,d^3Z = m\,n\,4\pi\,dz &= \left[\rho\,d^3V\right]_{PNC} \\ &= \left[\rho\frac{4\pi R^2 R'}{\sqrt{1+2E}}\,dr\right]_{PNC} \\ mn &= \hat{\rho}\,\frac{\hat{R}^2\widehat{R'}}{\sqrt{1+2E}}\,\frac{dr}{dz} \end{aligned}$$

From the above we derive DEs for extracting the LT model from the data, i.e. DEs for the 3 arbitrary functions $M(z)$, $E(z)$, $t_B(z)$ [9]:

$$\frac{dr}{dz} = \phi \ , \qquad \frac{d\phi}{dz} = \phi\left\{\frac{1}{(1+z)} + \frac{\frac{d^2\hat{R}}{dz^2} + \frac{4\pi mn\phi}{\hat{R}}}{\frac{d\hat{R}}{dz}}\right\}$$

$$\frac{dM}{dz} = \frac{4\pi mn\sqrt{1+2E}}{\phi} \qquad \text{where} \qquad \sqrt{1+2E} = \frac{\frac{d\hat{R}}{dz}}{2\phi} + \frac{\left(1 - \frac{2M}{\hat{R}}\right)\phi}{2\frac{d\hat{R}}{dz}}$$

The right hand sides of the DEs all contain the unknown functions *and* the observational data. In addition, there is an algebraic equation for $t_B(z)$.

1.6. *Four Integration Regions*

In practice, there are regions that need different treatments, illustrated in the $\hat{R}$ vs z plot below (for a RW model)

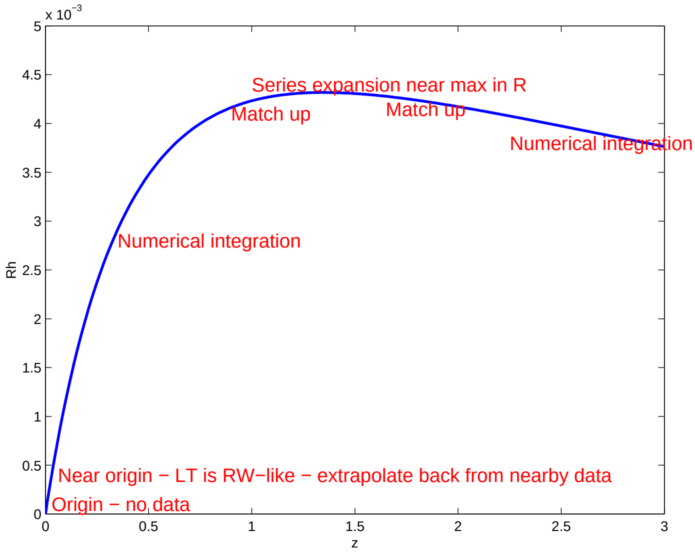

(a) Origin: There is no actual data at the origin, and very little near it, but the DEs need initial values at the origin. However, the origin of an LT model is RW-like, so we use the first few data points to extrapolate back to the origin.
(b) Inner region: The DEs are integrated numerically.
(c) Maximum: Near the maximum in $\hat{R}(z)$ the DEs go singular, so we do series expansion about R_{max} and join it to the end of the numerical run.
(d) Outer region: The DEs are again integrated numerically.
Each region must be matched properly to the next.

1.7. *The Maximum in* $\hat{R}(z)$

At the maximum we have $\frac{d\hat{R}}{dz} = 0$ and it is evident that the above DEs become singular. Actually this problem occurs even if the observations are exactly RW, and is a generic feature of any integration method. It would probably be worse in non spherical symmetry. We do a series expansion about R_{max}, which occurs at z_m:

$$\begin{aligned}
\hat{R} &= \hat{R}_m - \hat{R}_2\delta z^2 + \hat{R}_3\delta z^3 + \cdots \\
mn &= (mn)_m + (mn)_1\delta z + (mn)_2\delta z^2 + \cdots \\
M &= M_m + M_1\delta z + M_2\delta z^2 + \cdots \\
\phi &= \phi_m + \phi_1\delta z + \phi_2\delta z^2 + \cdots \\
\sqrt{1+2E} \; = W &= W_m + W_1\delta z + W_2\delta z^2 + \cdots
\end{aligned}$$

where $\delta z = (z - z_m)$, and insert these into the DEs, which to zero & first order give

$$\phi_1 = \frac{\hat{R}_m}{4\pi(mn)_m}\left(\frac{\hat{R}_2}{(1+z)} - 3\hat{R}_3 - \frac{(mn)_1\hat{R}_2}{(mn)_m}\right)$$

$$M_m = \frac{\hat{R}_m}{2}\ , \qquad M_1 = M_1\ , \qquad W_m = \frac{M_1}{4\pi(mn)_m}$$

$$W_1 = \frac{M_2}{4\pi(mn)_m} + \frac{R_2}{8\pi(mn)_m} + \frac{M_1\phi_1}{2R_mR_2} + \frac{3M_1R_3}{8\pi(mn)_mR_2} - \frac{2\pi(mn)_m}{R_m}$$

We see that all the ϕ coefficients are determined, but the M and W coefficients all depend on either W_m or M_1, which are not determined. However, the numerical integration has already given us M_a and $(dM/dz)_a$ at some point z_a before z_m, i.e.

$$M_a = M_m + M_1(z_a - z_m) + M_2(z_a - z_m)^2 + \cdots$$

$$\left(\frac{dM}{dz}\right)_a = M_1 + 2M_2(z_a - z_m) + \cdots$$

so we can solve for M_1 and M_2.

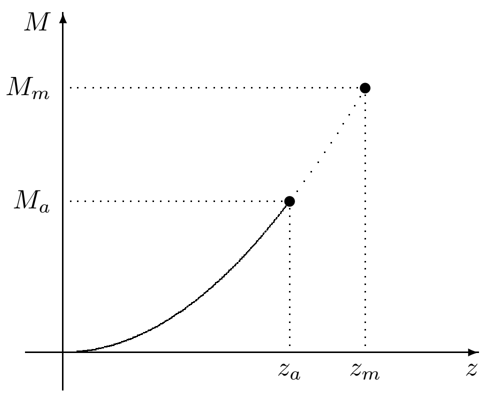

1.8. *Results*

The above numerical procedure was run for a range of fake data, including open, nearly-flat, and closed homogeneous models and a variety of mildly and strongly inhomogeneous models. We here plot the comparison of output functions with original functions for a strongly inhomogeneous model. The graphs below show the accuracy of the results for a strongly inhomogeneous model, showing M vs z, $W = \sqrt{1+2E}$ vs z, and respectively.

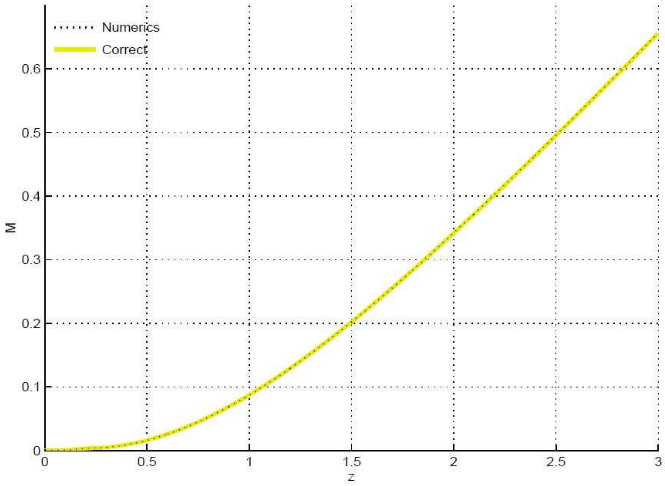
Numerics
Correct
M
z

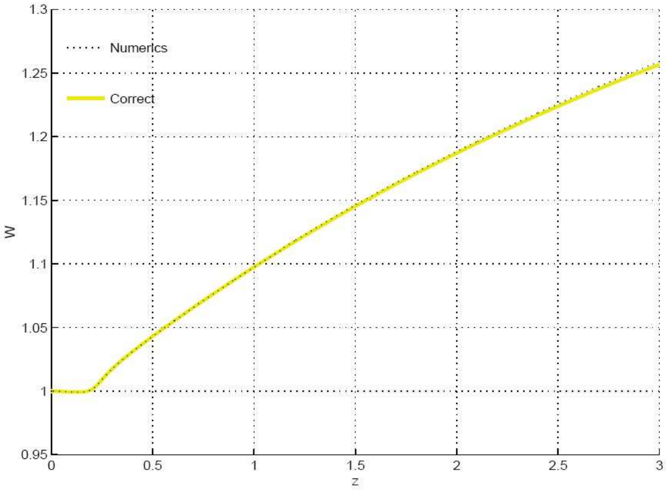
Numerics
Correct
W
z

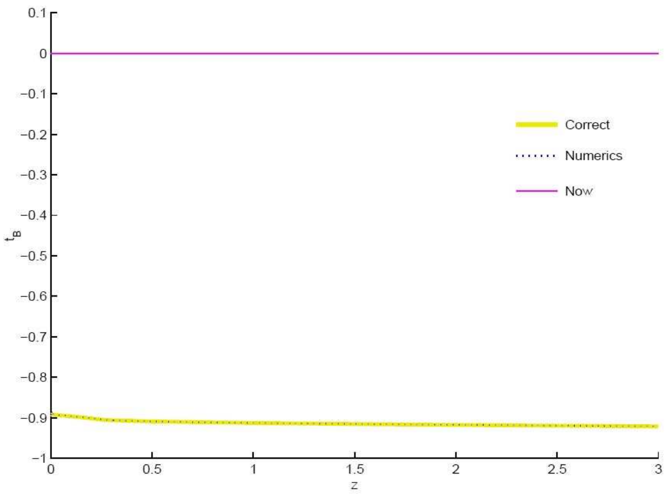

In each case agreement of the output functions (M, E & t_B) with those of original model was good to excellent. Not surprisingly, the function with the largest discrepancy was $W = \sqrt{1+2E}$. In some cases there was a noticeable discrepancy near the origin in τ and t_B, indicating an imperfect estimate of the origin parameters.

1.9. *Conclusions - Metric of Cosmos*

We have successfully implemented the MHE algorithm, and demonstrated its viability. It was tested with fake data, for many homogeeous & inhomogeneous models. The accuracy quite good, with E having the highest error, as might be expected.

The reduction of actual data is underway — this is for practice only, as much larger quantities of much more accurate data is needed. Many improvements & extensions to the method will be needed. We are gaining experience with reducing cosmological data, in anticipation of a flood of cosmological data.

Knowing the nearby metric will assist in analysing distant observations in more than just a statistical sense. Eventually we'll be able to quantify the degree of homogeneity, and won't have to *assume* homogeneity.

2. Measuring a Characteristic Mass of the Cosmos

We here point out a significant characterisation of the cosmos on giga-parsec scales that will become measurable with the next generation of surveys. The insight here is in putting together long-known results, not in the maths itself. As is well known, for objects of a given physical size, there is a maximum in the areal radius of our past null cone (PNC), i.e. a minimum in the apparent size.

2.1. *Mass, Radius and Apparent Horizon*

The gravitational mass M within comoving radius r, used in calculating light bending, orbital velocities, etc, is not the same as the integrated density on a constant t section, i.e. the sum of the rest masses of galaxies, gas clouds, dark matter concentrations, etc,

$$M = \int \rho \, dV = \int \frac{M'}{\sqrt{1+2E}} \, dr \ .$$

The derivative of R down the PNC,

$$\frac{d}{dr}\hat{R} = \Big[\dot{R}\,\hat{t}' + R' \Big]_{PNC} = \left[\left(\frac{-\dot{R}}{\sqrt{1+2E}} \ + \ 1 \right) R' \right]_{PNC}$$

in terms of physically measureable quantities is

$$\frac{d\hat{R}}{dz} = \frac{\hat{R}'}{z'} = \left[\frac{R'}{\dot{R}'(1+z)} \left(\sqrt{1+2E} \ - \dot{R} \right) \right]_{PNC} \ , \qquad \frac{d\hat{R}}{dz}\bigg|_{origin} \to \left[\frac{R'}{\dot{R}'} \right]_{r=0}$$

For there to be a maximum in $\hat{R}(z)$, $d\hat{R}/dz$ must go through zero as $\dot{R}$ inceases to the past. The apparent horizon (AH) is the locus of all such points — for all PNCs in observer's history:

$$\sqrt{1+2E} \ = \dot{R} = \sqrt{\frac{2M}{R} + 2E + \frac{\Lambda R^2}{3}} \qquad \to \qquad 2M = R - \frac{\Lambda R^3}{3}$$

Thus the maximum in d_D is where our PNC crosses the AH.

2.2. *Significance of the Maximum in* $\hat{R}$

This maximum in $d_D = \hat{R}$ is (a) a distinctive feature of an observational plot, (b) a characteristic of the cosmos we inhabit and the time we observe it, and (c) it determines the gravitational mass contained within that radius.

$$2M_m = \hat{R}_m - \frac{\Lambda \hat{R}_m^3}{3} \ , \qquad \text{where} \qquad \Lambda = 3H_0^2 \Omega_\Lambda$$

There are two roots: the smaller, at $\hat{R}_m$, is the AH; the larger, at $\hat{R}_m$, is the de Sitter horizon. Any given worldline (at constant M_m) either encounters both or neither. This is illustrated below for a family of incoming light rays in a homogeneous model, with $H0 = 70$, $\Omega_m = 0.3$, $\Omega_\Lambda = 0.7$.

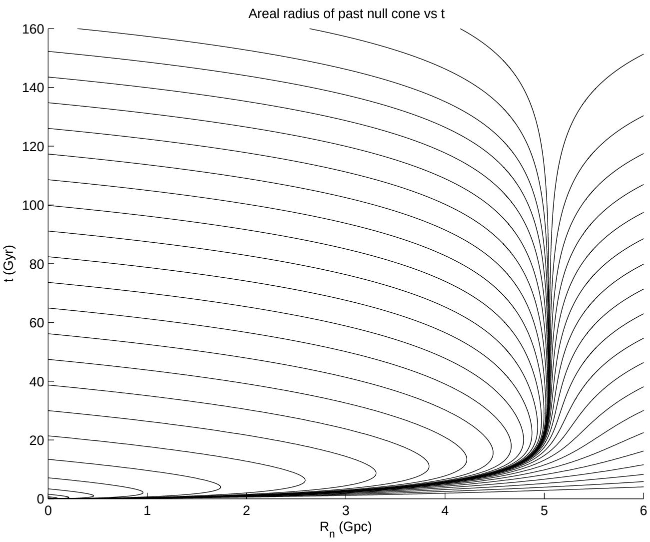

The $\hat{R}$-z Curves for families of RW models with Ω_m varying, with Ω_Λ varying, and with H_0 varying can be seen in [10]. The curves are most sensitive to variations in Ω_Λ & H_0 near z_m, the maximum in $\hat{R}$, and have close to maximum sensitivity to Ω_m variations there too. In addition, variations in Ω_Λ, H_0, and Ω_m move the maximum in very different directions.

2.3. *Conclusions - Mass of the Cosmos*

• The next generation of surveys should determine $\hat{R}_m$ and z_m quite well.
• A determination of $\hat{R}_m$ and Λ will fix the cosmic mass M_m on giga-parsec scales, even in inhomogeneous universe, i.e. *independently* of whether homogeneity is assumed or not. This is not true for any other point on our PNC.
• For the RW model, determination of $\hat{R}_m$ & z_m puts constraints on Ω_m, Ω_Λ, H_0.
• This result provides an amendment to the MHE theorem — the total mass from mn and the mass deduced from $\hat{R}_m$ *must mesh correctly* here — the observations $n(z)$, $\ell(z)$ & $\delta(z)$, plus the evolution functions $m(z)$, $L(z)$ & $D(z)$ plus the Λ value must satisfy the AH eq.
• Key features of $\hat{R}$-z curve — the location of the maximum & the initial slope — $\hat{R}_m$, z_m & H_0 — define a natural "best fit" or "average" FLRW model. This definition is based on geometry, but uses observations.
• A determination of $\hat{R}_m$ and z_m is likely to be the first observational detection of a relativistic horizon.

References

1. J. Kristian and R.K. Sachs (1966) *Astrophys. J.* **143**, 379-99, "Observations in Cosmology".
2. G.F.R. Ellis, S.D. Nel, R. Maartens, W.R. Stoeger, & A.P. Whitman (1985) *Phys. Reports* **124**, 315-417, "Ideal Observational Cosmology".

3. C. Hellaby (2003) Mathematics of Gravitation II, Warsaw, September 2003, http://www.impan.gov.pl/Gravitation/ConfProc/, "Finding the Metric of the Cosmos".
4. N. Mustapha, C. Hellaby and G.F.R. Ellis (1997) *Mon. Not. Roy. Astron. Soc.* **292**, 817-30, "Large Scale Inhomogeneity Versus Source Evolution: Can We Distinguish Them Observationally?".
5. G. Lemaître (1933) *Ann. Soc. Sci. Bruxelles* **A53** 51-85; reprinted in *Gen. Rel. Grav.* **29**, 641-80 (1997).
6. R.C. Tolman (1934) *Proc. Nat. Acad. Sci.* **20** 169-76, reprinted in *Gen. Rel. Grav.* **29**, 935-43 (1997).
7. C. Hellaby & K. Lake, *Astrophys. J.* **282**, 1 (1984); and errata in *Astrophys. J.* **294**, 702 (1985)
8. C. Hellaby, *Class. Q. Grav.* **4**, 635-50 (1987)
9. H.-C. Lu, C. Hellaby, *in preparation* (2005).
10. C. Hellaby, (2006) *Mon. Not. Roy. Astron. Soc.* **370**, 239-244, "The Mass of the Cosmos".